Journal of Quantitative Spectroscopy & Radiative Transfer 261 (2021) 107486

Contents lists available at ScienceDirect

Journal of Quantitative Spectroscopy & Radiative Transfer

journal homepage: www.elsevier.com/locate/jqsrt

The foreign-continuum absorption of water vapour in the far-infrared (50–500 cm^{-1})

Aleksandra O. Koroleva[a], Tatyana A. Odintsova[a], Mikhail Yu. Tretyakov[a], Olivier Pirali[b,c], Alain Campargue[d,*]

[a] Institute of Applied Physics, Russian Academy of Sciences, 46 Ul'yanov St, Nizhniy Novgorod, 603950, Russia
[b] Université Paris-Saclay, CNRS, Institut des Sciences Moléculaires d'Orsay, Orsay 91405, France
[c] SOLEIL Synchrotron, L'Orme des Merisiers, Saint-Aubin 91192, Gif-Sur-Yvette, France
[d] Univ. Grenoble Alpes, CNRS, LIPhy, Grenoble 38000, France

ARTICLE INFO

Article history:
Received 8 July 2020
Revised 17 December 2020
Accepted 17 December 2020

Keywords:
Water vapour
Rotational spectrum
In-band continuum
Bimolecular absorption
Terahertz gap
Synchrotron

ABSTRACT

We investigated the continuum absorption of water vapour diluted in nitrogen, oxygen and air in the range of the pure rotational band of the water molecule (50-500 cm^{-1}). Spectra recordings were performed at room temperature with a Fourier transform spectrometer associated to a 151-m multipass gas cell located at the AILES beamline of SOLEIL synchrotron facility. The study includes the first laboratory measurements in the wide 90-330 cm^{-1} interval. Tests of the baseline stability, crucial for the continuum determination, are reported together with the expected pressure dependences of the continuum absorption, measured over different pressure ramps. Retrieved foreign-continuum cross-sections are found in good agreement with literature values available in the lower and upper parts of the studied frequency range. The reported results validate the MT_CKD foreign-continuum empirical model, widely used in atmospheric applications, even if some overestimation of the MT_CKD values is noted in the centre of the band where experimental data were absent.

1. Introduction

Appropriate calculations of radiation balance, modelling of global climate changes, and atmosphere remote sensing require an accurate quantification of atmospheric absorption in the whole electromagnetic spectrum. The far-infrared region (usually defined as radiation within frequency range of about 0.3 – 20 THz or 10 – 700 cm^{-1}) is of particular interest for atmospheric sciences. The far-infrared (IR) region contains resonance lines of the major and minor atmospheric constituents, such as O_2, NO_2, O_3, NH_3, CO_2 but water vapour, in spite of its relatively small atmospheric abundance (~1%), is the dominant contributor to the absorption of both incoming solar and outgoing thermal radiation [1–3]. In the global average, the latter has maximum in the far IR range near 560 cm^{-1}. In general, line parameters (centre frequency, intensity, pressure-shift and -broadening coefficients) of these molecules as listed in current spectroscopic databases (*e.g.* HITRAN [4]) are known and can be used in remote sensing experiments.

In addition to resonance lines, atmospheric absorption includes a weak non-resonant continuum absorption (or just *continuum*), smoothly varying with frequency. Intermolecular interactions during collisions are known as physical origin of the continuum. At atmospheric conditions, pair interactions dominate over higher order effects (triple, quadruple, *etc.*) so the continuum absorption can be considered as a result of bimolecular interactions.

Atmospheric continuum can be subdivided into a water-related component (wet continuum) and a dry component (mostly due to the interaction of nitrogen and oxygen molecules with each other). The wet continuum can be in turn divided into two contributions corresponding to interaction of water molecules with each other (*self-continuum*) and with other atmospheric molecules (*foreign-continuum*). It is known that the larger the dipole moments of collisional partners (or the next term of multipole expansion of charge distribution for non-polar molecules) are, the larger the continuum magnitude is. Water molecule possesses dipole moment of 1.85 D that leads to a strong self-continuum.

Foreign water vapour continuum in air originates predominately from interaction of H_2O molecules with the two most abundant atmospheric gases: nitrogen and oxygen. Being symmetric diatomic molecules, neither O_2 nor N_2 possess an electric dipole moment. That is why H_2O-N_2 and H_2O-O_2 foreign continuum cross-sections are significantly weaker than the H_2O-H_2O

* Corresponding author.
E-mail addresses: koral@ipfran.ru (A.O. Koroleva), odintsova@ipfran.ru (T.A. Odintsova), trt@ipfran.ru (M.Yu. Tretyakov), olivier.pirali@universite-paris-saclay.fr (O. Pirali), alain.campargue@univ-grenoble-alpes.fr (A. Campargue).

https://doi.org/10.1016/j.jqsrt.2020.107486
0022-4073/

self-continuum cross-sections. Nevertheless, in usual conditions, the high concentration of O_2 and N_2 makes both the foreign- and self-continua have an appreciable effect in the atmosphere.

The wet continuum amplitude is very small compared to the absorption at the centre of resonance lines. Nevertheless, due to its wide spectral extension, its contribution to the total atmospheric absorption has significant impact on the greenhouse effect [3]. The far IR dry air continuum component, corresponding mostly to interactions between O_2 and N_2 molecules can be generally neglected in normal and wet atmospheric conditions because the corresponding bimolecular absorption cross-section is about one order of magnitude weaker than H_2O foreign-continuum cross-section [5].

The continuum absorption is poorly studied in the far IR not only because of its weakness, but also because of the well known difficulties of efficient generation and detection of radiation in this spectral range, sometimes called the "THz gap" (see, *e.g.* review in [6]). The present contribution is part of a series of laboratory studies of the water vapour continuum using synchrotron-based Fourier transform spectroscopy (FTS) technique. The self-continuum absorption was first investigated in the 10-650 cm^{-1} range [7–9]. This range covers most part of the H_2O pure rotational band, thus the studied continuum can be classified as an *in-band* continuum. The derived cross-sections together with the results of previous investigations by Burch (350-800 cm^{-1}) [10] indicated that the MT_CKD model [11–13], commonly used in radiative transfer codes, overestimates the magnitude of the self-continuum in the considered range by about 30%. The present work is devoted to a similar study and validation test of the MT_CKD foreign-continuum. Previous laboratory measurements of the foreign-continuum were reported in the low- (3.5-84.1 cm^{-1}) [14–18] and high- (337.9-629.0 cm^{-1}) [19] frequency wings of the H_2O band, missing the range where the band and the related continuum reach their maximum. It should be mentioned, however, that foreign-continuum retrieval was performed over the entire spectral range from atmospheric emitted (downwelling) spectral radiance observations [12,20–22]. These atmospheric measurements are, on one hand, quite sensitive because of the long atmospheric path but on the other hand, their accuracy is limited by uncertainties related to the atmospheric model and poorly controlled environmental conditions. Nevertheless, these data provide the major experimental constraints to the MT_CKD continuum coefficients in the far IR [12].

The goal of the present work is thus a laboratory determination of the H_2O foreign-continuum cross-sections associated with dry air, nitrogen and oxygen in the 50-500 cm^{-1} frequency range. The measurements of O_2- and N_2-cross-sections allow us to check the consistency with the separate determination of the air cross-sections. In Section 2, we give a brief description of the experimental setup and spectra acquisition. The details of the data analysis are given in Section 3. Section 4 presents the experimental results, their discussion and comparison with previously known data. The conclusions are summarised in Section 5. Additional information on the data analysis and the retrieved cross-section data are given in *Supplementary Materials*.

2. Experimental set-up

The experimental approach is very similar to that used in [8]. The FTS spectra of wet atmospheric gases (nitrogen, oxygen and dry air) were recorded at room temperature (296±1.5 K, permanently monitored by PT100 thermo-sensors attached to the gas cell) at the AILES beamline of the SOLEIL synchrotron using a FT spectrometer (Bruker IFS-125HR) associated to a multipass White-type cell with the total optical pathlength $L = 151.75 \pm 1.5$ m. The synchrotron radiation extracted by the AILES beamline of SOLEIL facility (operating in the 500-mA standard multibunch mode) allowed recording absorption spectra in the 50-700 cm^{-1} spectral interval. Additional experiments were performed in the same spectral range with a globar source providing much lower power in comparison to the synchrotron radiation. The light intensity transmitted through the absorption cell was measured using a liquid He cooled Si bolometer.

The absorption coefficient was determined as $\alpha_{total} = (1/L)\ln(I_0(\nu)/I(\nu))$, where $I(\nu)$ and $I_0(\nu)$ correspond to the signal when the cell was filled with the mixture of water vapour and foreign gas (studied spectrum) and with a non-absorbing gas (reference spectrum or baseline), respectively. Typical examples of $I(\nu)$ and $I_0(\nu)$ recordings performed under the same experimental conditions using globar and synchrotron sources of far-IR radiation are presented in Fig. 1.

Prior to the measurements of foreign continuum absorption spectra, recordings with pure N_2 were performed at different pressures to test the baseline stability. They revealed some pressure induced baseline variations, notable for wavenumbers above 300 cm^{-1}. These variations are assigned to the deformation of the gas cell windows made of thin film (polypropylene, 50 μm). These changes were almost reproducible after pumping out and re-filling the cell at the same pressure in the range up to about 400 mbar (presumably due to an elastic deformation of the windows). Higher pressures resulted in significant and non-reproducible baseline variation (inelastic deformation). Consequently, the maximum value of the pressure was limited to 400 mbar. More details on the baseline stability tests are provided as *Supplementary Materials* attached to this paper.

Five series of spectra were recorded in the experimental conditions summarized in Table 1. The reference spectra providing the baseline were recorded at the beginning of each series.

Each series included two steps. First, the cell was filled with a given pressure of water vapour and then the foreign gas (N_2, O_2 and dry air for series 1-3, 4 and 5, respectively) was gradually injected up to the maximum (total) pressure. Spectra were recorded at various pressure steps of the pressure ramp. Then the gas mixture was pumped out and additional spectra were recorded for various pressure values during the decreasing pressure ramp. Note that during the filling with the foreign gas, the partial pressure of

Table 1
Experimental conditions.

Foreign gas	Nitrogen			Oxygen	Dry air
Gas purity, %	99.9999			99.9995	99.999
Radiation source	Globar	Synchrotron			
Series number	1	2	3	4	5
Number of pressure points	9	10	8	9	8
Filling H_2O pressure, mbar	3	2	4	4	4
Min./max. total pressure, mbar	20/100	40/200	100/430	200/400	200/400
Number of acquisitions	200 - 400	200	100 - 200	200	200

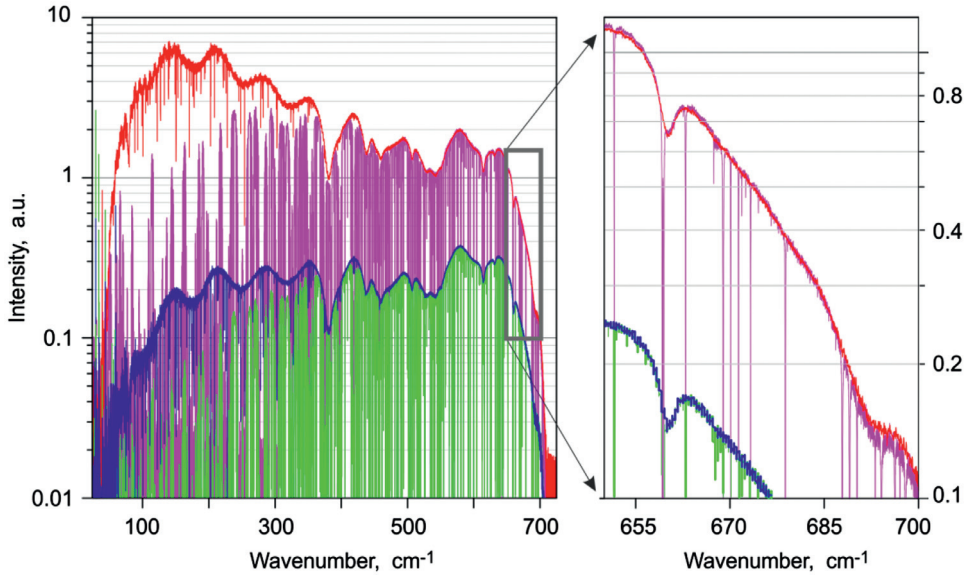

Fig. 1. Typical example of raw FTS spectra for a mixture of 96 mbar of nitrogen and 4 mbar of water vapour (pink) recorded using the synchrotron radiation and corresponding reference spectrum recorded with 100 mbar of pure N_2 (red). Similar recordings with the globar source (green and blue, respectively). The right panel shows a zoom of the 655-700 cm^{-1} region.

water vapour is supposed to be constant while when the gas mixture is pumped out, the relative concentration of water vapour is expected to be constant and thus water vapour partial pressure decreases proportionally to the total pressure.

The gas pressure was measured by three complementary sensors (Pfeifer, 10, 100 and 1000 mbar, uncertainty 0.25 % of reading). As mentioned above, for each wet gas spectrum, the reference spectrum was recorded with the corresponding dry foreign gas at the same pressure in order to minimize the baseline change. The remaining minor changes of the baseline (see insert in Fig. 1, near 700 cm^{-1}) were taken into account by introducing an empirical adjustable parameter as discussed in the next section.

Resonance lines due to water vapour present as an impurity are clearly observed in the reference spectrum (Fig. 1). Corresponding water content was estimated to be less than 0.005 mbar. Such small amount of residual water does not notably impact the resulted continuum value and can be neglected.

The wet (studied) and dry (reference) spectra were recorded with a spectral resolution of 0.02 and 0.2 cm^{-1}, respectively. The resolution of 0.02 cm^{-1} is comparable to the width of the resonance lines at the pressure conditions of the recordings; thus as checked in our previous studies [7–9], instrumental spectral function does not notably affect the magnitude of the continuum retrieved between resonance lines (micro-windows of transparency) and is not taken into account in the data treatment presented below.

3. Data treatment

The retrieved absorption coefficient, α_{total}, is considered as the sum of the resonance lines, α_{res}, and of the continuum absorption, α_{cont}:

$$\alpha_{total}(\nu, P_{H_2O}, P_{for}) = \alpha_{res}(\nu, P_{H_2O}, P_{for}) + \alpha_{cont}(\nu, P_{H_2O}, P_{for}), \quad (1)$$

where ν is frequency, P_{H_2O} and P_{for} are water vapour and foreign gas partial pressure, respectively.

Resonant absorption was modelled as a line-by-line sum of H_2O lines with the following profile [23]:

$$\alpha_{Line} = \frac{S}{\pi} R(\nu) \left(\frac{\Delta\nu_c}{(\nu - \nu_0)^2 + \Delta\nu_c{}^2} + \frac{\Delta\nu_c}{(\nu + \nu_0)^2 + \Delta\nu_c{}^2} \right), \quad (2)$$

where

$$\Delta\nu_c = \Delta\nu_{H_2O} + \Delta\nu_{for} = P_{H_2O}\ \gamma_{H_2O} + P_{for}\ \gamma_{for}, \quad (3)$$

and

$$R(\nu) = \frac{\nu}{\nu_0} \frac{\tanh(h\nu/2kT)}{\tanh(h\nu_0/2kT)}, \quad (4)$$

where $\Delta\nu_c$ is the collisional width of the line, γ_{H_2O} and γ_{for} are self- and foreign-gas pressure broadening coefficients, respectively. Note that the Doppler line width at our experimental conditions in the frequency range under consideration is less than $\Delta\nu_c$ by at least 2 orders of magnitude and can be neglected. We also neglected the resonance spectrum of O_2 because it is very weak [24] and mostly removed automatically because the reference spectrum is recorded with dry O_2 at the same pressure. Frequencies (ν_0), line strengths (S), self- and air-broadening coefficients were taken from the HITRAN2016 database [4]. Water lines pressure broadening by nitrogen and oxygen were taken from the results of calculations [25,26]. Nitrogen broadening coefficients were calculated for the three most abundant water isotopologues ($H_2{}^{16}O$, $H_2{}^{18}O$ and $H_2{}^{17}O$) for the transitions in the ground vibrational state involving values of the total angular momentum quantum number J lower than 23. In [26], oxygen broadening coefficients are provided for the pure rotational transitions of the main isotopologue, $H_2{}^{16}O$, with $J < 10$. For all other ground state lines we used air-broadening coefficients from HITRAN2016 multiplied by the average ratio of air- to foreign gas (over all lines for which these coefficients are known), broadening, which was found to be 1.064(57) and 0.67(10) for N_2- and O_2-broadening, respectively. General consistency between used broadening parameters was verified assuming that $\gamma_{air} = 0.79\gamma_{N_2} + 0.21\gamma_{O_2}$ (see *Supplementary Materials* for details). For the other H_2O isotopologues and rotational transitions in vibrationally excited states, the broadening coefficients were assumed to be the same as for the $H_2{}^{16}O$ corresponding lines in the ground state. [27,28].

The standard far-wing cut-off at 25 cm^{-1} from the line centre was applied, the far wings of the line below and above the cut-off frequency being excluded and the remaining almost rectangular absorption (the “pedestal” or “plinth”) underneath the modelled line profile being preserved as an intrinsic part of the resonance absorption.

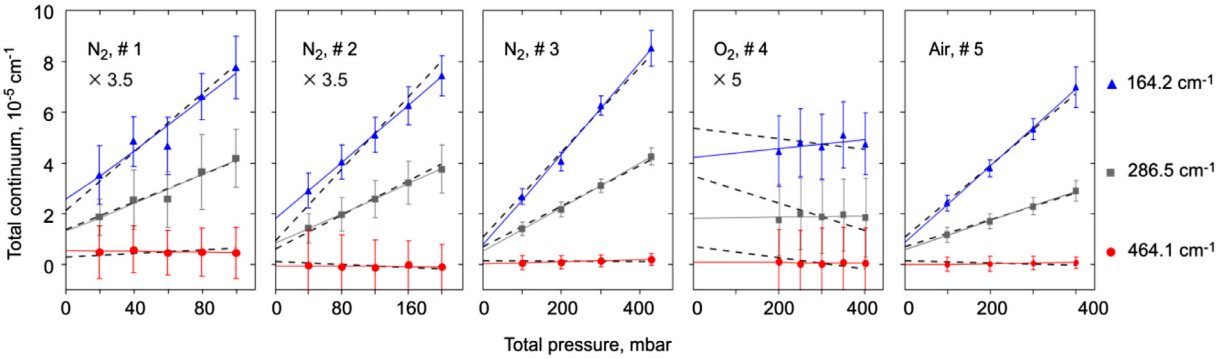

Fig. 2. Total derived continuum absorption in H_2O-N_2, H_2O-O_2 and H_2O-air mixtures *versus* total gas pressure for three typical micro-windows during increasing pressure ramps. The absorption magnitude for Series 1-2 and 4 have been multiplied by 3.5 and 5 respectively. Error bars correspond to 1σ standard deviation of the noisy signal from its mean value within the current micro-window. Solid and dashed straight lines correspond to the best fit of linear function with and without the empirical correction term $\Delta\alpha$, to the same points (see text for details).

Total continuum absorption, α_{cont}, was determined by subtracting the calculated resonance absorption, α_{res}, from the measured absorption coefficient, α_{total}. Considering the fact that baselines were recorded with the cell filled with the foreign gas at the same pressure as the one adopted for the wet gas recordings, α_{cont} does not include the dry continuum contribution and is thus the sum of the two wet components, namely the self- α_{self} and α_{for} , respectively:

$$\alpha_{cont}(\nu, P) = \alpha_{self}(\nu, P) + \alpha_{for}(\nu, P) = C_s P_{H_2O}^2/kT + C_f P_{H_2O} P_{for}/kT. \quad (5)$$

In this formula, C_s and C_f are the self- and foreign-continuum cross-sections (in $cm^2 molecule^{-1} atm^{-1}$), respectively, P is the total pressure of the mixture $P = P_{H_2O} + P_{for}$.

The continuum absorption, $\alpha_{cont}(\nu, P_{H_2O}, P_{for})$, was determined within as many as possible manually selected micro-windows of transparency between resonance water lines. Most of the selected micro-windows coincide with those considered in our previous studies of the self-continuum [8,9].

3.1. Increasing pressure ramps

During the filling with the foreign gas, the partial pressure of water vapour in the gas is assumed to be independent of the amount of foreign gas injected in the cell. In this case the self-continuum absorption remains invariant. The foreign-continuum absorption and thus the total continuum absorption are expected to increase linearly with the total gas pressure (Eq. (5)). This is indeed reflected by the obtained pressure dependences (Fig. 2).

The self- and foreign-continuum cross-sections were determined as the fitted values of the intercept at zero and slope of the foreign gas pressure dependences (Eq. (5)), respectively. Error bars relative to C_s and C_f were obtained as the statistical errors provided by the fit weighted according to the uncertainty of each measurement point. The latter corresponds to one standard deviation of the noisy absorption spectra from its mean value within the current micro-window. Note that the uncertainties related to measured pressure and temperature values are negligible. We checked that the self-continuum cross-sections retrieved from different series of measurement coincide within the 3σ error bars. As illustrated in Fig. 3, although less accurate, the weighted average values of the five different C_s determinations are found consistent with the C_s values of [9] derived from pure water vapour spectra. C_f values retrieved from the increasing pressure ramp measurements are provided as *Supplementary Materials* for the five series. They are considered as preliminary information which will be validated and discussed in comparison with corresponding values obtained from decreasing pressure ramps.

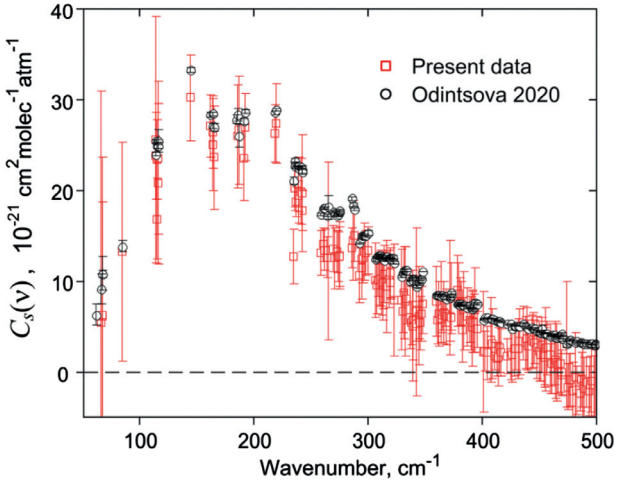

Fig. 3. Water vapour self-continuum cross-section averaged over all data retrieved in this work from increasing pressure ramps (open red squares) and similar data from [9] (open black circles). Error bars correspond to 1σ uncertainty.

The achieved agreement allows us to use the C_s values of Odintsova et al. [9] to subtract the calculated self-continuum component from the total measured continuum. In accordance with Eq. (5), the remaining part is due to the foreign continuum. In these conditions, we expect a higher accuracy of C_f retrieval by using C_s values of [9] in each experimental series. However, some deviations including quasiperiodic low frequency variations of the retrieved C_s around the C_s values of [9] are notable in Fig. 3. These deviations, assigned to the remaining baseline variations (see *Supplementary Materials*), can be corrected by introducing an empirical frequency dependent correction term, $\Delta\alpha(\nu)$, which is used as an adjustable parameter when fitting the model to the experimental data:

$$\alpha_{for}(\nu, P) = \alpha_{cont}(\nu, P) - C_s^{Odintsova} P_{H_2O}^2/kT = \Delta\alpha(\nu) + C_f P_{H_2O}/kT \quad (6)$$

Note that the baseline variations, corrected by the introduction of $\Delta\alpha$, may have different instrumental origins including not only incomplete compensation of the interference fringes with pressure variations, but other sources such as drift of the mean source power.

The impact of $\Delta\alpha$ can be seen in Fig. 2 as a deviation between solid and dashed lines, the latter corresponding to $\Delta\alpha = 0$. Both

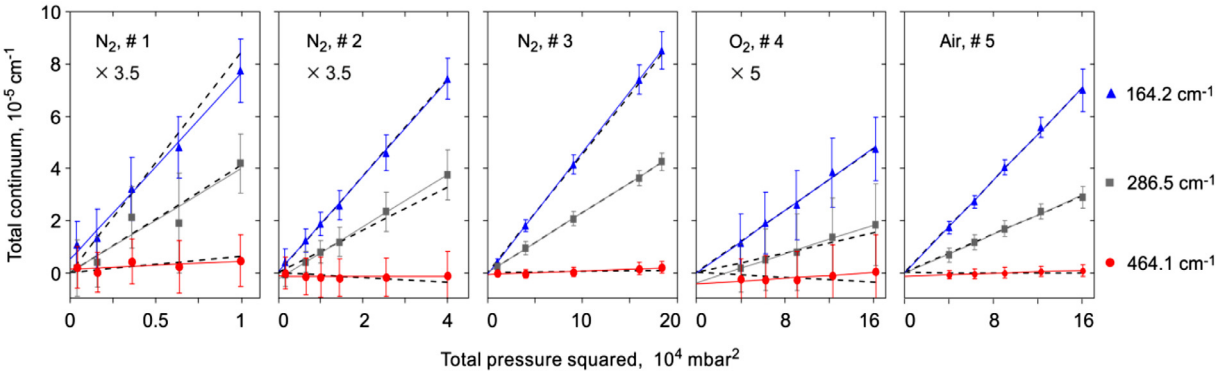

Fig. 4. Total derived continuum absorption in H_2O-N_2, H_2O-O_2 and H_2O-air mixtures *versus* total gas pressure squared for measurement points in three typical micro-windows at decreasing pressure ramps. The absorption magnitude for Series 1-2 and 4 have been multiplied by 3.5 and 5 respectively. Error bars correspond to 1σ standard deviation of the noisy signal from its mean value within the current micro-window. Solid and dashed straight lines correspond to the best fit with and without the empirical correction term $\Delta\alpha$ (see text for details).

lines are well within the uncertainty range of experimental points but, in average, over all micro-windows the introduction of the correction term improves the *rms* of the linear fit by a factor of 3. Under the experimental conditions chosen in this work, the correction term is from about 10 to 100 times smaller than the total continuum absorption. More details on the correction term magnitude, its impact on the retrievals of the continuum and its potential relation to the water vapour amount variations are given in *Supplementary Materials*. Note that $\Delta\alpha(\nu)$ is independent of the pressure and thus C_f derived at the same time as deriving the C_s from these data (*i.e.* ignoring values of [9]) is the same as deriving it using the formalism of Eq. (6) in the case of the increasing pressure ramp. However, we introduce the $\Delta\alpha$ correction term at this step because it is required for the proper data treatment of the decreasing pressure ramps.

3.2. Decreasing pressure ramps

The volume fraction (relative concentration) of water vapour in the cell is assumed to be unchanged during the pumping out of the gas mixture. Thus the P_{H_2O}/P ratio is constant and Eq. (5) can be modified as follows:

$$\alpha_{cont}(\nu, P) = \Delta\alpha(\nu) + \beta(\nu)P^2/kT, \tag{7}$$

including the aforementioned adjustable parameter $\Delta\alpha$ corresponding to the remaining variations of the baseline and

$$\beta(\nu) = C_s^{Odintsova}\left(\frac{P_{H_2O}}{P}\right)^2 + C_f\left(\frac{P_{H_2O}}{P}\right)\left(1 - \frac{P_{H_2O}}{P}\right), \tag{8}$$

which is constant within each micro-window. Thus, during the pumping out, the amplitude of the continuum absorption is expected to decrease proportionally to the total gas pressure squared. This is indeed confirmed by the experimental results displayed in Fig. 4. Dashed and solid straight lines are for $\Delta\alpha$ set to zero and variable, respectively. In the latter case, the deviation of the fit averaged over all micro-windows is improved by a factor of 2.7 (see *Supplementary Materials* for details).

The foreign-continuum cross-sections were calculated from β values derived from the linear dependence of $\alpha_{cont}(\nu,P)$ *versus* P^2 using C_s values from [9]. C_f error bars correspond to the statistical uncertainty of the weighted fit of β taking into account the uncertainty of each measurement point. The uncertainty of C_f related to C_s error bar was found to be more than an order of magnitude smaller that the aforementioned statistical uncertainty and was neglected. The uncertainties related to measured pressure and temperature values at this experimental step are also negligible.

Fig. 5 shows the good agreement between the C_f determinations derived from the increasing and decreasing pressure ramps for all series. The retrieved values coincide within measurement uncertainty, validating the data treatment procedure. Large measurement uncertainty in Series 1 is explained by smaller radiation power available from the globar source than from the synchrotron (Fig. 1) and in Series 2 by small amount of water vapour (Table 1), leading in both cases to smaller signal-to-noise ratio compared to other series. Periodic variations of the difference are seen for Series 3 and 4. These variations are similar to those shown in the lower part of Fig. S1 provided in the Supplementary Material. The similarity indicates an imperfect elimination of the baseline change by the correction term $\Delta\alpha$. This can be understood as different baselines were used for different pressures, whereas the term takes into account only common variations for all data points.

The C_f values determined from the decreasing pressure ramps are provided as *Supplementary Material*. In the remaining part of the paper, we will use mean weighted values from the increasing and decreasing pressure ramps for comparison with literature data.

The C_f values related to the H_2O-N_2 continuum were obtained from three experimental series (No. 1-3 in Table 1) performed under different conditions (H_2O relative concentration and radiation sources). The comparison of the three series of derived C_f values is displayed in Fig. 6. Series 1 corresponding to the globar radiation source leads to systematically higher values. Nevertheless, the three sets of data agree within the 3σ measurement uncertainty. The mean weighted values of C_f from all of the three series are provided as *Supplementary Material* as our final derived set of H_2O-N_2 continuum cross-sections. The provided measurement error (evaluated as 68.26% confidence interval) thus includes not only the statistical uncertainty related, for example, to the detector noise in a single spectrum recording, but also a value resulting (in the case of H_2O-N_2 continuum) from the analysis of 27 spectra together with the same number of baselines. So the provided error value takes into account possible systematic effects related in particular to different gas mixtures, different radiation sources and the baseline variations due to both pressure drops and/or radiation power drift.

The H_2O-O_2 continuum turned out to be too weak to be determined in our experimental conditions (Fig. 6). Only an upper limit of 10^{-22} $cm^2molec^{-1}atm^{-1}$ (to be compared to a maximum H_2O-N_2 C_f value of about 2×10^{-21} $cm^2molec^{-1}atm^{-1}$) can be reported. Large spread of points and negative cross-sections are due to uncertainties of pressure broadening parameters (see *Supplementary Materials* for details). This is confirmed by the good coincidence of the H_2O-O_2 C_f values determined from increasing

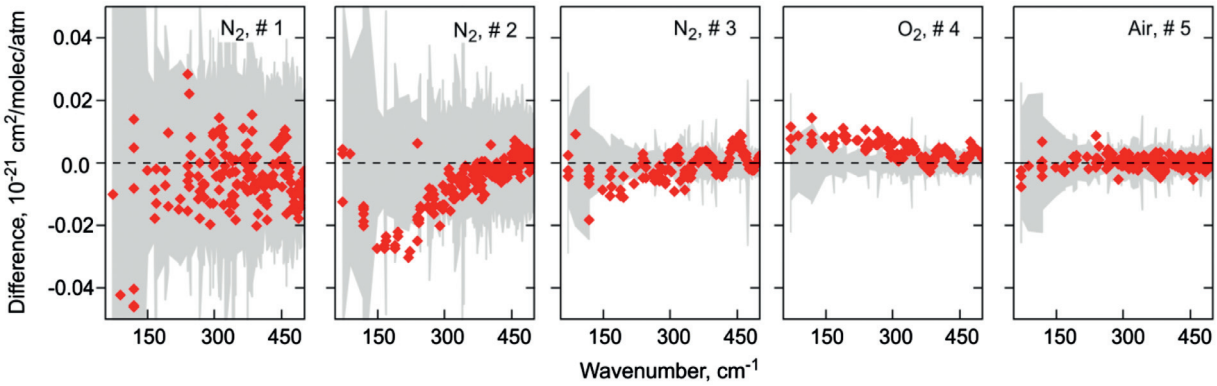

Fig. 5. Differences between the retrieved C_f values corresponding to the increasing and decreasing pressure ramps. Grey areas represent $\pm 1\sigma$ combined uncertainty of two datasets centered on zero.

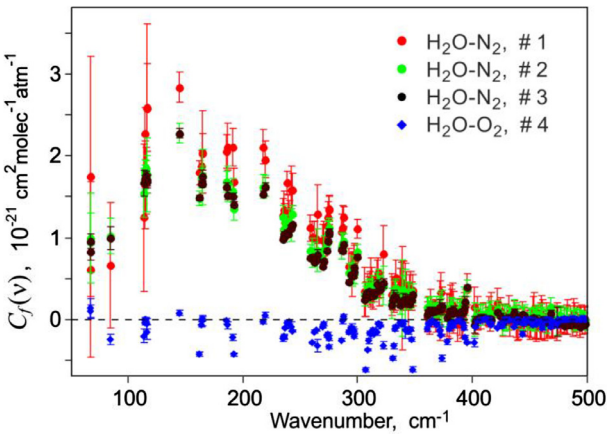

Fig. 6. Cross-sections of H_2O-N_2 and H_2O-O_2 foreign-continuum absorption averaged over increasing and decreasing pressure ramps. Error bars correspond to 1σ combined uncertainty of the two datasets.

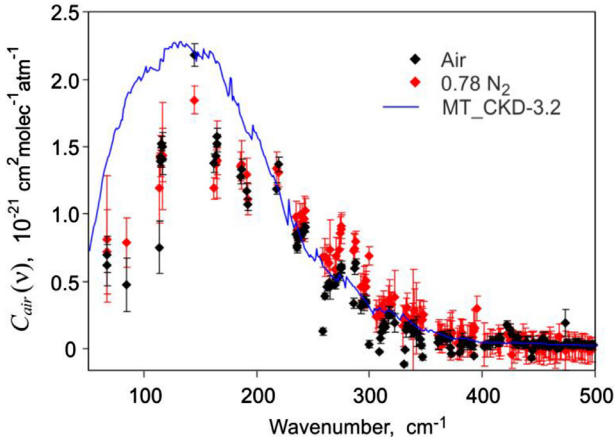

Fig. 7. H_2O-air (red rhombs) and multiplied by 0.78 H_2O-N_2 (black rhombs) foreign-continuum cross-sections retrieved in this work. Error bars correspond to 1σ uncertainty. Solid line presents corresponding data of MT_CKD-3.2 for comparison. Irregular fluctuations of this line are due to the resonance line pedestals removal from the continuum (see text for details).

and decreasing pressure ramps (Fig. 5). This agreement is several times better than the amplitude of the fluctuations between successive micro-windows indicating that these fluctuations are mostly due to inaccuracies in the subtraction of the resonance absorption resulting from an insufficient knowledge of the pressure broadening coefficients.

The H_2O-O_2 continuum results can be used to check the consistency of the H_2O-N_2 and H_2O-air cross-sections, as discussed in the next section.

4. Discussion

Water vapour foreign-continuum in the Earth atmosphere is due to molecular collisions of water molecules with nitrogen (78.084 %), oxygen (20.95 %) and argon (0.934 %):

$$\alpha_{H_2O-air} = C_{H_2O-air} P_{H_2O} \frac{P_{air}}{kT} = C_{H_2O-N_2} P_{H_2O} \frac{P_{N_2}}{kT} + C_{H_2O-O_2} P_{H_2O} \frac{P_{O_2}}{kT} + C_{H_2O-Ar} P_{H_2O} \frac{P_{Ar}}{kT}, \quad (9)$$

where C_{H_2O-air}, $C_{H_2O-N_2}$, $C_{H_2O-O_2}$ and C_{H_2O-Ar} are corresponding foreign-continuum cross-sections.

The contribution of H_2O-Ar pairs to the atmospheric continuum absorption is expected to be small not only because of the small relative abundance of argon but also because of the properties of Ar as a collisional partner. For example, the H_2O-Ar cross-section in the millimetre wavelength range was measured to be several times less than the H_2O-N_2 cross-section [29]. We thus consider that the H_2O-Ar contribution to the air absorption continuum is negligible ($C_{H_2O-Ar} = 0$). As shown in the previous section, the H_2O-O_2 continuum was too weak to be determined ($C_{H_2O-O_2} = 0$), which led to the simple relation:

$$C_{H_2O-air} = 0.78 C_{H_2O-N_2}. \quad (10)$$

Fig. 7 illustrates the good agreement between the measured C_{H_2O-air} values and those calculated using Eq. (10) and the measured $C_{H_2O-N_2}$ cross-sections. Systematic deviations can be noted in the range 250-400 cm^{-1}. In our opinion, they are related to the inaccuracy of H_2O lines foreign-broadening parameters. The deviations are prominent in this particular range because the number of micro-windows is increasing towards high frequencies while the number of intense water lines influencing the continuum magnitude decreases. For further comparison with literature data (below), our final derived C_{H_2O-air} values corresponding to the mean weighted from our N_2 and air data, provided as Supplementary Materials, will be used.

Before comparing our continuum with previous data, we would like to remind readers that the continuum magnitude depends directly on the list of resonance lines used to simulate the monomer absorption (in particular their pressure broadening parameters). For a proper comparison, the same line list and the same method of resonance absorption calculations should be used. Considering the number of sources, as well as the possible lack of traceability

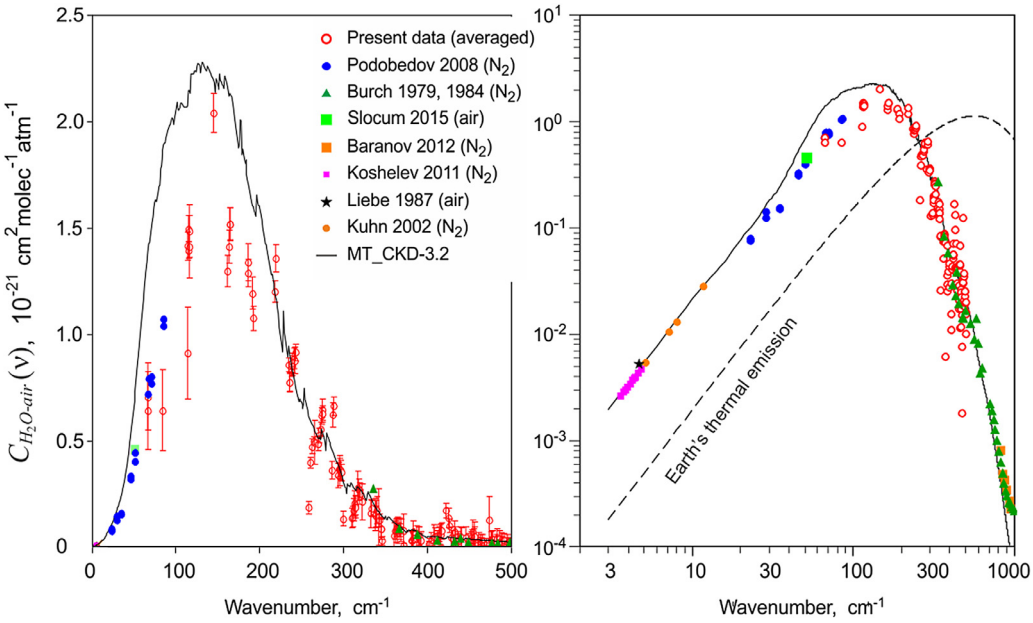

Fig. 8. Comparison of the present results to literature laboratory data on absorption cross-sections of the H_2O-air continuum at 296 K in linear (left) and logarithmic (right) scales. Weighted average values of H_2O-N_2 and H_2O-air data from this work (Fig. 7) are shown by red circles. Measurements with H_2O-N_2 mixtures from [18,31] (dark green triangles) and [17] (blue filled circles) are multiplied by 0.78 (Eq. (10)). Moist air measurements from [29] are shown by bright green square. Other known microwave and IR data from [14–16,32] below and above studied range are shown for comparison by different symbols (see legend in the figure). The MT_CKD-3.2 model foreign continuum is displayed by black solid curve. The dotted curve in the right panel is the Planck's law for the Earth's mean thermal emission radiance (in arbitrary units).

of the used line parameters, a detailed comparison of C_f data is a tedious work which should be the subject of a dedicated study. We provide as part of the *Supplementary Material* a discussion of the possible impact of the used resonance line list to the derived foreign continuum. Thus, the following comparison should be considered only as a preliminary discussion of the data obtained in the present work.

Three previous laboratory studies can be used for comparison with our results:

(i) The H_2O-N_2 foreign continuum absorption was investigated within 7 micro-windows in the range of 22-84 cm^{-1} at 293, 313 and 333 K [17]. For comparison, all these data were extrapolated to 296 K using temperature exponent derived in [17] and scaled using Eq. (10). It should be mentioned, that far-wing cut-off at 100 cm^{-1} from the line centre was applied for the resonance absorption model in [17]. So for comparison with our results, the cumulative contribution of resonance line wings within the 25-100 cm^{-1} range of detuning from the line centres were added to the continuum reported in [17].

(ii) Extended series of room temperature measurements of water vapour in air was reported in a narrow interval near 50 cm^{-1} [30]. Significant variation of experimental conditions (optical path length, composition and pressure of the mixture) allowed quite reliable determination of the H_2O-air continuum.

(iii) Finally, Burch performed a systematic experimental study of the H_2O-N_2 continuum in the ranges 338-629 cm^{-1} [19] and 720-1000 cm^{-1} [31].

These previous experimental data and our final derived C_{H_2O-air} values are gathered in Fig. 8 and compared to the MT_CKD-3.2 foreign-continuum model. It should be recalled, that the MT_CKD continuum includes the "pedestal" (the trapezoid underneath the line profile subtracted from the resonance absorption) [11]. For the proper comparison of the experimental data with the MT_CKD model, we subtracted the cumulative pedestal of the H_2O rotational spectrum from the model spectrum. Note that the latter modification decreases the model continuum by about 25% in the range of the maximum of the H_2O band and introduces non-smoothness of the spectrum, which is seen even in logarithmic scale of the figure. A good overall agreement is obtained with previous measurements available in the low- and high-frequency wings of the H_2O band. The agreement with the MT_CKD-3.2 [13] model is very good in the range above 200 cm^{-1} although the model overestimates the continuum in the in-band region (60-200 cm^{-1}) where previous measurements were absent.

Note that this overestimation is slightly larger than the continuum deviation caused by the choice of the line list (AER or HITRAN). It is nevertheless well within the limits of C_f variation related to water line pressure broadening parameter uncertainties (see *Supplementary Materials* for details).

The results of other known laboratory studies related to the H_2O-air foreign continuum are presented in Fig. 8 including datasets retrieved at lower and higher frequencies than our work. Additionally, we plotted in the figure the black-body spectral radiance curve (Planck's law) for a temperature 287 K corresponding to the mean thermal emission of the Earth and demonstrating the importance of the considered spectral range for the radiation budget of our planet. As the maximum of the thermal emission curve is close to the range of the H_2O-air continuum maximum, the continuum uncertainty directly affects the corresponding uncertainty of the outgoing energy.

5. Conclusion

The foreign-continuum absorption of moist nitrogen, oxygen and air has been investigated using synchrotron-based Fourier transform spectroscopy at room temperature in the 50-500 cm^{-1} frequency range. Cross-section values were derived from the pressure dependence of the measured absorption for series of pressure values during increasing and decreasing pressure ramps. The oxygen contribution to the foreign continuum of water vapour in air is found to be mostly negligible compared to the N_2 contribution.

The foreign continuum in air is thus limited to the N_2 contribution and a good consistency is obtained between the results obtained with air and with N_2.

To the best of our knowledge, the reported results are the first laboratory study of water vapour foreign-continuum covering the entire spectral range of the H_2O rotational band. Our data on the water vapour foreign-continuum are consistent with earlier experimental results of Podobedov [17] and Burch [19] in the lower and upper parts of the studied spectral range, respectively, and in general confirm the validity of the MT_CKD model widely used for atmospheric applications.

Declaration of Competing Interest

The authors declare that they have no known competing financial interests or personal relationships that could have appeared to influence the work reported in this paper.

CRediT authorship contribution statement

Aleksandra O. Koroleva: Formal analysis, Methodology, Writing - original draft. **Tatyana A. Odintsova:** Data curation, Investigation, Methodology. **Mikhail Yu. Tretyakov:** Conceptualization, Data curation, Writing - review & editing. **Olivier Pirali:** Data curation, Resources, Methodology. **Alain Campargue:** Formal analysis, Validation, Writing - review & editing.

Acknowledgement

This work became possible thanks to the Project No. 20180347 supported by SOLEIL Synchrotron Team. Experimental part of the work was performed under partial financial support from the RFBR research project No. 18-55-16006. Resonance absorption modelling and continuum data analysis were funded by RFBR within the research projects No. 18-02-00705 and No. 18-05-00698, respectively.

Supplementary materials

Supplementary material associated with this article can be found, in the online version, at doi:10.1016/j.jqsrt.2020.107486.

References

[1] Clough SA, Iacono MJ, Moncet J-L. Line-by-line calculations of atmospheric fluxes and cooling rates: application to water vapour. J Geophys Res 1992;97/D14:15761–85.
[2] Harries JE. Physics of the Earth's radiative energy balance. Contemp Phys 2000;41(5):309–22. doi:10.1080/001075100750012803.
[3] Shine KP, Ptashnik IV, Rädel G. The water vapour continuum: brief history and recent developments. Surv Geophys 2012;33:535–55. doi:10.1007/s10712-011-9170-y.
[4] Gordon IE, Rothman LS, Hill C, Kochanov RV, Tan Y, Bernath PF, et al. The HITRAN2016 molecular spectroscopic database. J Quant Spectrosc Radiat Transf 2017;203:3–69.
[5] Boissoles J, Boulet C, Tipping RH, Brown A, Ma Q. Theoretical calculation of the translation-rotation collision-induced absorption in N_2–N_2, O_2–O_2, and N_2–O_2 pairs. J Quant Spectrosc Radiat Transf 2003;82:505–16.
[6] Consolino L, Bartalini S, De Natale P. Terahertz frequency metrology for spectroscopic applications: a review. J Infrared Millim Te 2017;38:1289–315. doi:10.1007/s10762-017-0406-x.
[7] Odintsova TA, Tretyakov MYu, Pirali O, Roy P. Water vapour continuum in the range of rotational spectrum of H_2O molecule: new experimental data and their comparative analysis. J Quant Spectrosc Radiat Transf 2017;187:116–23.
[8] Odintsova TA, Tretyakov MYu, Zibarova AO, Pirali O, Roy P, Campargue A. Far-infrared self-continuum absorption of $H_2{}^{16}O$ and $H_2{}^{18}O$ (15–500 cm^{-1}). J Quant Spectrosc Radiat Transf 2019;227:190–200.
[9] Odintsova TA, Tretyakov MYu, Simonova AA, Ptashnik IV, Pirali O, Campargue A. Measurement and temperature dependence of the water vapour self-continuum between 70 and 700 cm^{-1}. J Mol Struct 2020;1210:128046. doi:10.1016/j.molstruc.2020.128046.
[10] Burch DE. Continuum absorption by H_2O; 1982. Report No AFGL-TR-81-0300.
[11] Mlawer EJ, Payne VH, Moncet JL, Delamere JS, Alvarado MJ, Tobin DC. Development and recent evaluation of the MT_CKD model of continuum absorption. Philos Trans R Soc A 2012;370:2520–56.
[12] Mlawer EJ, Turner DD, Paine SN, Palchetti L, Bianchini G, Payne VH, Cady-Pereira KE, Pernak RL, Alvarado MJ, Gombos D, Delamere JS, Mlynczak MG, Mast JC. Analysis of water vapour absorption in the far-infrared and submillimeter regions using surface radiometric measurements from extremely dry locations. J Geophys Res-Atmos 2019;124(14):8134–60.
[13] https://doi.org/10.1098/rsta.2011.0295. Continuum model, (n.d.) http://rtweb.aer.com/continuum_frame.html (accessed December 15, 2020)].
[14] Koshelev MA, Serov EA, Parshin VV, Tretyakov MY. Millimeter wave continuum absorption in moist nitrogen at temperatures 261–328 K. J Quant Spectrosc Radiat Transf 2011;112:2704–12.
[15] Liebe HJ, Layton DH. Millimeter-wave properties of the atmosphere: laboratory studies and propagation modeling; 1987. NTIA Report. No. 87-224.
[16] Kuhn T, Bauer A, Godon M, Buehler S, Kuenzi K. Water vapour continuum: absorption measurements at 350 GHz and model calculations. J Quant Spectrosc Radiat Transf 2002;74:545–62.
[17] Podobedov VB, Plusquellic DF, Siegrist KE, Fraser GT, Ma Q, Tipping RH. New measurements of the water vapour continuum in the region from 0.3 to 2.7 THz. J Quant Spectrosc Radiat Transf 2008;109:458–67.
[18] Podobedov VB, Plusquellic DF, Siegrist KE, Fraser GT, Ma Q, Tipping RH. Continuum and magnetic dipole absorption of the water vapour—oxygen mixtures from 0.3 to 3.6 THz. J Quant Spectrosc Radiat Transf 2008;251:203–9.
[19] Burch DE, Gryvnak DA. Method of calculating H_2O transmitting between 333 and 633 cm^{-1}; 1979. Report No AFGL-TR-79-0054.
[20] Green PD, Newman SM, Beeby RJ, Murray JE, Pickering JC, Harries JE. Recent advances in measurement of the water vapour continuum in the far-infrared spectral region. Philos Trans Ser A Math Phys Eng Sci 2012;370(1968):2637–55. doi:10.1098/rsta.2011.0263.
[21] Liuzzi G, Masiello G, Serio C, Palchetti L, Bianchini G. Validation of water vapour continuum absorption models in the wave number range 180–600 cm^{-1} with atmospheric emitted spectral radiance measured at the Antarctica Dome-C site. Opt Express 2014;22(14):16784–801. doi:10.1364/OE.22.016784.
[22] Shi S-C, Paine S, Yao QJ, Lin ZH, Li XX, Duan WY, et al. Terahertz and far-infrared windows opened at Dome A in Antarctica. Nat Astron 2016;1(1):1–7. doi:10.1038/s41550-016-0001.
[23] Clough SA, Kneizys FX, Davies RW. Line shape and water vapor continuum. Atmos Res 1989;23:229–41.
[24] Toureille M, Béguier S, Odintsova TA, Tretyakov MYu, Pirali O, Campargue A. The O_2 far-infrared absorption spectrum between 50 and 170 cm^{-1}. J Quant Spectrosc Radiat Transf 2020;242:106709. doi:10.1016/j.jqsrt.2019.106709.
[25] Vispoel B, Cavalcanti JH, Gamache RR. Modified complex Robert-Bonamy calculations of line shape parameters and their temperature dependence for water vapour in collision with N_2. J Quant Spectrosc Radiat Transf 2019;228:79–89.
[26] Gamache, R. Private communication, 2019.
[27] Gamache RR, Fischer J. Half-widths of $H_2{}^{16}O$, $H_2{}^{18}O$, $H_2{}^{17}O$, $HD^{16}O$, and $D_2{}^{16}O$: I. Comparison between isotopomers. J Quant Spectrosc Radiat Transf 2003;78:289–304.
[28] Gamache RR, Hartmann J-M. Collisional parameters of H_2O lines: effects of vibration. J Quant Spectrosc Radiat Transf 2004;83:119–47.
[29] Bauer A, Godon M, Carlier J, Gamache RR. Continuum in the windows of the water vapour spectrum. Absorption of H_2O-Ar at 239 GHz and linewidth calculations. J Quant Spectrosc Radiat Transf 1998;59(3-5):273–85.
[30] Slocum DM, Giles RH, Goyette TM. High-resolution water vapour spectrum and line shape analysis in the terahertz region. J Quant Spectrosc Radiat Transf 2015;159:69–79.
[31] Burch DE, Alt RL. Continuum absorption by H_2O in the 700–1200 cm^{-1} and 2400–2800 cm^{-1} windows, MA, USA: Hanscom Air Force Base; 1984. US Air Force Geophysics Laboratory report AFGL-TR-84–0128.
[32] Baranov Yu I, Lafferty WJ. The water vapour self- and water–nitrogen continuum absorption in the 1000 and 2500 cm^{-1} atmospheric windows. Philos Trans R Soc A 2012;370:2578–89.